

# Research on an improved UWB space location method

CHENGBO HU<sup>1,4</sup>, XIAOBO WANG<sup>1</sup>, YONGLING LU<sup>1</sup>,  
WEIHUA CHENG<sup>2</sup>, WEI DAI<sup>3</sup>

**Abstract.** Because of its strong anti-multipath capability and other characteristics, UWB technology is widely used in positioning. While using UWB, unstable phenomenon of the positioning results still remained. In this paper, we proposed an improved UWB space location method. We first proposed a distance optimization method and then introduced the distance intersection of space method which uses three base stations to solve spatial location. The experimental results show that the proposed method is simple and easy to implement. Besides, it is with small computation cost and high accuracy of positioning. At the same time, because the method only needs three base stations to measure the three-dimensional coordinate of the tested point, it can save the hardware cost to a certain extent. Finally, this method is suitable for warehouse location and other scenes.

**Key words.** UWB, ranging optimization, distance intersection of space method.

## 1. Introduction

At present, location information has become an important basis for the development of all walks of life. GNSS (GPS, GLONASS, BDS, Galileo) ensures the efficient and convenient realization of outdoor positioning. With the development of wireless communication technology, emerging technologies, such as Bluetooth, WiFi, ZigBee and UWB, have played an important role in indoor positioning, and they make up for the shortcomings that GNSS cannot work in the indoor and other complex environments. UWB [1] is a low-power, low-cost but high-speed wireless communication technology. Recently, UWB positioning technology has been extensively researched by researchers. Normal operating frequency of UWB is between 3.0 GHz to 10.6 GHz [2]. UWB is characterized by not using carrier communication, but with very short time interval (nanosecond or less than nanosecond time interval) of the baseband

---

<sup>1</sup>Jiangsu Electric Power Company Research Institute, Nanjing, 211167, China

<sup>2</sup>Jiangsu Power Info-tech Co. Ltd., Nanjing, 211167, China

<sup>3</sup>Jiangsu BDS Application Industry Institute, Nanjing, 211167, China

<sup>4</sup>Corresponding author

narrow pulse communication, with penetrating power, anti-multipath effect of anti-interference ability outstanding. Especially, in the metal or liquid environment that have great impact on signal attenuation, UWB plays a stronger performance than other wireless positioning technology [3]. In view of the outstanding characteristics of UWB technology, many scholars use UWB technology for positioning research. The key to achieve high-precision positioning is to obtain high-precision ranging data through UWB. According to the characteristic parameters used in UWB ranging, UWB ranging methods include RSS (Received Signal Strength), AOA (Angle of Arrival), TOA (Time of Arrival) TDOA (Time Difference of Arrival) measurement [4]. In [5], AOA, TOA, and TDOA are considered to be the focus of attention. Typical algorithms are based on the arrival time of UWB direct path components. Works [6–7] studied the direct path, and analyzed the multi-path resolution. The range data were divided into LOS (Line of Sight) and NLOS (Not Line of Sight), two types. In order to get high accuracy positioning results, many scholars have studied the algorithm of coordinate solution. Currently, Chan algorithm [8], Fang algorithm [9] and least square algorithm [10] are usually used. These algorithms are based on the improvement of the algorithm itself, and they do not take the optimal data type into account. In addition, these algorithms do not make full use of data for the location of quasi-real-time applications. In this paper, a method of 2-second data preprocessing of continuous time data is proposed. The method makes full use of the high-frequency characteristics of UWB technology. The method is simple and feasible and easy to implement. At the same time, the method can determine the three-dimensional coordinates of the tags with only three base stations, thus saving the hardware cost of the UWB module. Besides, it is applicable to the application scenario where the real-time requirement is not very high.

## 2. Modeling of underwater robot kinematics

### 2.1. Positioning system

United States Time Domain P440 module are used as both base station and tag in positioning platform. This product is with superior performance, and it has a good anti-multipath effect, and can achieve high-precision ranging. Between the module and the module can achieve two-way communication ranging. At the same time, the operating frequency of the module can also be artificially set. Three modules are used as the base station of the UWB positioning platform, one module is used as the label of the UWB positioning platform. Thus three-dimensional coordinates of the label are obtained by the three base stations.

### 2.2. Algorithmic flow

Because the module can realize the two-way communication distance measurement (TW-TOF), the range type of the positioning platform can be obtained by the formula

$$\text{Amount} = C_n^m, \quad (1)$$

where  $m$  is the total number of modules in the positioning platform, ( $m = 4$  in this platform), and  $n = 2$  because of two-way ranging. Then the normal range of the platform type is 6.

The flow of the algorithm is shown in Figure 1.

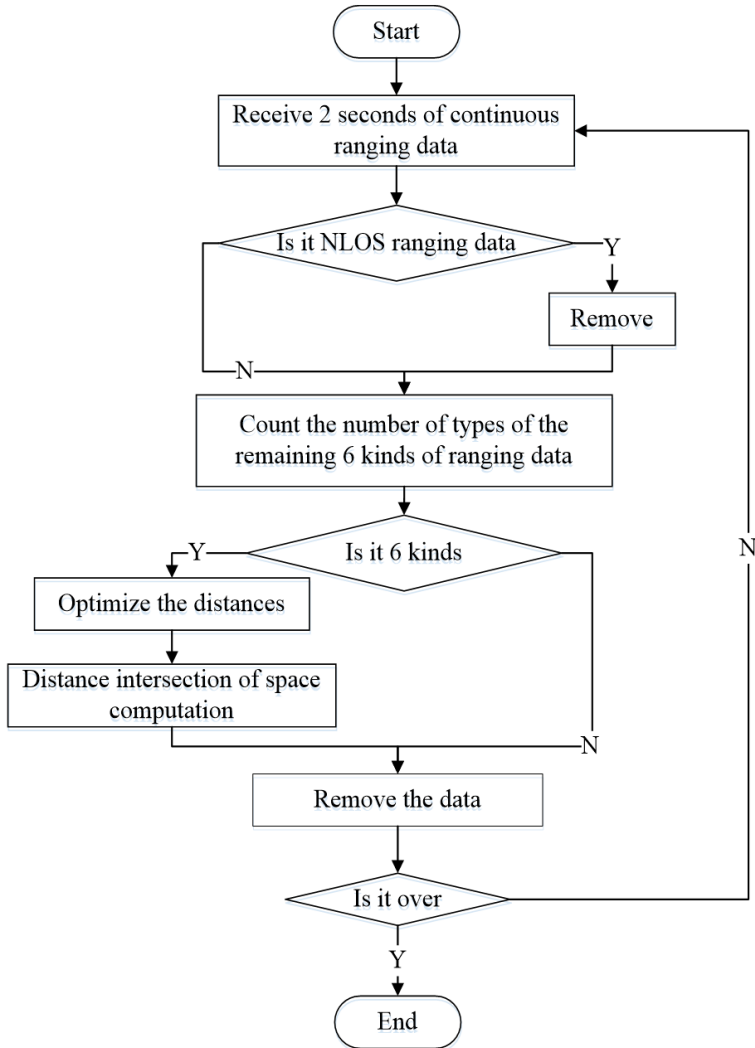


Fig. 1. Algorithm flowchart

First, the positioning platform receives the ranging data for two consecutive seconds, the interval time of the module is set to 10 ms. Thus the period of the six kinds of ranging polling is 60 ms, that is, 16.67 Hz. Therefore, about 33 ranging can be obtained theoretically for 2 seconds.

Then, it is judged whether or not NLOS type data is received for the received

ranging data. As the UWB actual communication can be effected by the external environment and its own stability. There are two types of data, LOS and NLOS. In the NLOS state, the TOA and TDOA data will produce the error of excessive time delay, so the direct use of the NLOS ranging data for spatial location will bring large error of positioning error [11]. If NLOS data exists, the NLOS data should be discarded.

After all processing is complete, the remaining data are all LOS type data. If there are 6 kinds of remaining data, there are 6 ranging information in the positioning platform, which can be used to optimize the edge distance, and then used in the follow-up space measurement; if the type is less than 6, it indicates that at least one kind of ranging type data in the ranging data is completely removed during the process of removing the NLOS type data, in which case the distance intersection of space can not be performed. Thus the data of the continuous 2 seconds is deleted. Then determine whether it is the end of the data. If not, continue to measure the range of data processing, otherwise go the end of the process.

### 3. Algorithm description

#### 3.1. NLOS type range determination

As described above, NLOS-type ranging data need to be eliminated because the error of the NLOS-type ranging value is large and it can leads a low positioning accuracy.

Based on the premise that the standard deviation of the NLOS data is greater than the standard deviation of the LOS data, the standard deviation of the actual range data is compared with the standard deviation of the LOS environment to determine whether the measurement period contains NLOS error [7].

At time  $t_i$ , the distance from the base station A to the tag is as shown in the formula

$$r_m(t_i) = r_m^0(t_i) + n_m(t_i) + \text{NLOS}_m(t_i), \quad (2)$$

where  $r_m^0(t_i)$  is the measurement distance determined by the LOS signal,  $n_m(t_i)$  is the system noise caused by the ranging error and  $\text{NLOS}_m(t_i)$  is the NLOS error distance.

Since  $\text{NLOS}_m(t_i)$  is always a nonnegative random variable, let  $\text{NLOS}_m(t_i)$  be a range of  $0 \leq \text{NLOS}_m(t_i) \leq \beta_m$ . And because  $n_m(t_i)$  obeys the normal distribution whose average value is 0, its value range is  $-\alpha_m \leq n_m(t_i) \leq \alpha_m$ , and then error scope of NLOS type range survey data is shown in the formula.

$$-\alpha_m \leq \text{NLOS}_m(t_i) + n_m(t_i) \leq \alpha_m + \beta_m. \quad (3)$$

Compared to the LOS type, the error becomes significantly larger, that is,  $\alpha_{\text{mNLOS}} < \alpha_{\text{mLOS}}$ . Then NLOS data can be judged.

As P440 module outputs range measurement data, it also outputs data type of the range data. Based on this feature, this positioning algorithm can extract the

data to solve.

### ***3.2. Optimization of measured distance***

The purpose of optimization of measured distance is to further eliminate NLOS data and improve the accuracy of ranging. The data collected for 2 consecutive seconds are processed to obtain the optimal distance in this period. The idea is as follows:

a) Obtain the data median  $N_1$  and average  $N_2$ . As the P440 module has a high ranging accuracy, the nominal ranging accuracy can reach 2 cm, and the data subject to normal distribution. So when the sample is sufficient,  $N_1$  is theoretically the same as  $N_2$ . Due to there are system errors during the actual processing process, there is some differences between  $N_1$  and  $N_2$ .

b) Judging by experience, the difference between  $N_1$  and  $N_2$  is set 0.01 m, that is 1 cm. If  $|N_1 - N_2| < 0.01$ , then the data is considered good, there is no large error value, the data obeys the normal distribution. We take  $N_1$  as the optimal distance value. If it is not satisfied, it is assumed that there is a ranging value containing the NLOS type value in the set of data.

Pauta Criterion is usually used in statistics to remove outliers [12]. It takes three times as error correction threshold of discrimination. Therefore, this paper, based on Pauta Criterion, proposed a method using  $N_1$  as the initial true value. In this way,  $N_1 \pm 3\sigma$  (standard deviation) is determined as decision interval of Pauta Criterion. The method uses the data in the interval to get its average value and takes it as the optimized ranging value.

### ***3.3. Optimization of measured distance***

At present, many scholars focus on the positioning of UWB in two-dimensional plane positioning [13], they lack the three-dimensional positioning of the label research.

The usual coordinates are solved by least squares [14]. The optimization of measured distance uses distance intersection of space method [15], which can be used to derive the three-dimensional coordinate of the label with three base stations.

The diagram of location is shown in Fig. 2.

In Fig. 2, A, B and C are the three base stations, P is the pending label. The relationship between A, B, C and P fits the law of the right hand, that is, when the right thumb is pointing to P, the other four fingers of the natural bending direction is A, B, C. It is to be noted that the three base stations cannot be located on the same straight line.

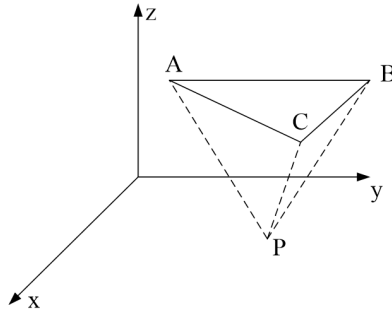


Fig. 2. Schematic diagram of location

Based on the spatial geometry, the volume formula of tetrahedral P-ABC is

$$V = \frac{1}{6} \begin{vmatrix} x_P - x_A & y_P - y_A & z_P - z_A \\ x_P - x_B & y_P - y_B & z_P - z_B \\ x_P - x_C & y_P - y_C & z_P - z_C \end{vmatrix} = \frac{1}{6} S_1 S_2 S_3 \begin{vmatrix} \cos \alpha_A & \cos \beta_A & \cos \gamma_A \\ \cos \alpha_B & \cos \beta_B & \cos \gamma_B \\ \cos \alpha_C & \cos \beta_C & \cos \gamma_C \end{vmatrix}, \quad (4)$$

where  $\cos \alpha_A$ ,  $\cos \beta_A$  and  $\cos \gamma_A$  represent the direction cosines of the vector AP,  $\cos \alpha_B$ ,  $\cos \beta_B$ ,  $\cos \gamma_B$  represent the direction cosines of the vector BP, and  $\cos \alpha_C$ ,  $\cos \beta_C$ ,  $\cos \gamma_C$  represent the direction cosines of the vector CP. Using  $K$  to represent the direction cosine matrix in formula (4), we obtain

$$V = \frac{1}{6} S_1 S_2 S_3 |K|. \quad (5)$$

We can obtain  $N$  as

$$N = |KK^T| = \sin^2 \varphi_{AB} + \sin^2 \varphi_{AC} + \sin^2 \varphi_{BC} + 2 \cos \varphi_{AB} \cos \varphi_{AC} \cos \varphi_{BC} - 2, \quad (6)$$

where:

$$|K| = \sqrt{\sin^2 \varphi_{AB} + \sin^2 \varphi_{AC} + \sin^2 \varphi_{BC} + 2 \cos \varphi_{AB} \cos \varphi_{AC} \cos \varphi_{BC} - 2} \quad (7)$$

Among them,  $\varphi_{AB}$ ,  $\varphi_{AC}$  and  $\varphi_{BC}$  are the angles between vectors PA and PB, vectors PA and PC, vectors PB and PC. The values of trigonometric function can be solved from triangles PAB, PAC and PBC.

Also define the vectors

$$\begin{aligned} \vec{AB} &= (x_B - x_A, y_B - y_A, z_B - z_A) = (X_B, Y_B, H_B), \\ \vec{AC} &= (x_C - x_A, y_C - y_A, z_C - z_A) = (X_C, Y_C, H_C), \\ \vec{AP} &= (x_P - x_A, y_P - y_A, z_P - z_A) = (X_P, Y_P, H_P). \end{aligned} \tag{8}$$

From the product of the inner product and the mixed product in formula (8), we can get

$$\left\{ \begin{aligned} &\left| \begin{array}{cc} Y_B & H_B \\ Y_C & H_C \end{array} \right| X_P + \left| \begin{array}{cc} H_B & X_B \\ H_C & X_C \end{array} \right| Y_P + \left| \begin{array}{cc} X_B & Y_B \\ X_C & Y_C \end{array} \right| H_P = M_1, \\ &X_B X_P + Y_B Y_P + H_B H_P = M_2, \\ &X_C X_P + Y_C Y_P + H_C H_P = M_3. \end{aligned} \right. \tag{9}$$

where  $M_1 = S_1 S_2 S_3 |K|$ ,  $M_2 = (D_{AB}^2 + S_A^2 - S_B^2)/2$ ,  $M_3 = (D_{AC}^2 + S_A^2 - S_C^2)/2$ , so the formula (9) can be solved, and we get

$$\left\{ \begin{aligned} X_P &= \frac{1}{\left| \begin{array}{cc} X_B & Y_B \\ X_C & Y_C \end{array} \right|} \left[ \left| \begin{array}{cc} Y_B & H_B \\ Y_C & H_C \end{array} \right| H_P - \left| \begin{array}{cc} Y_B & M_2 \\ Y_C & M_3 \end{array} \right| \right], \\ Y_P &= \frac{1}{\left| \begin{array}{cc} X_B & Y_B \\ X_C & Y_C \end{array} \right|} \left[ \left| \begin{array}{cc} H_B & X_B \\ H_C & X_C \end{array} \right| H_P - \left| \begin{array}{cc} M_2 & X_B \\ M_3 & X_C \end{array} \right| \right], \\ H_P &= \frac{M_1 \left| \begin{array}{cc} X_B & Y_B \\ X_C & Y_C \end{array} \right| + \left| \begin{array}{cc} Y_B & H_B \\ Y_C & H_C \end{array} \right| \left| \begin{array}{cc} Y_B & M_2 \\ Y_C & M_3 \end{array} \right| + \left| \begin{array}{cc} H_B & X_B \\ H_C & X_C \end{array} \right| \left| \begin{array}{cc} M_2 & X_B \\ M_3 & X_C \end{array} \right|}{\left| \begin{array}{cc} X_B & Y_B \\ X_C & Y_C \end{array} \right|^2 + \left| \begin{array}{cc} Y_B & H_B \\ Y_C & H_C \end{array} \right|^2 + \left| \begin{array}{cc} H_B & X_B \\ H_C & X_C \end{array} \right|^2}. \end{aligned} \right. \tag{10}$$

Then the three-dimensional coordinates of P point are  $x_P = X_P + x_A$ ,  $y_P = Y_P + y_A$ ,  $z_P = H_P + z_A$ .

### 4. Example analysis

Using the positioning method shown in Fig. 2. In the test environment, the label is placed on the metal surface, and there are fewer other obstacles in the environment. The improved spatial localization algorithm is validated and analyzed by MATLAB software.

#### 4.1. Analysis of measured distance optimization

We analyzed UWB modules' ranging data for two seconds. The results are shown in Fig. 3. In order to facilitate the distinction, the line which means not optimized is bold in Fig. 3.

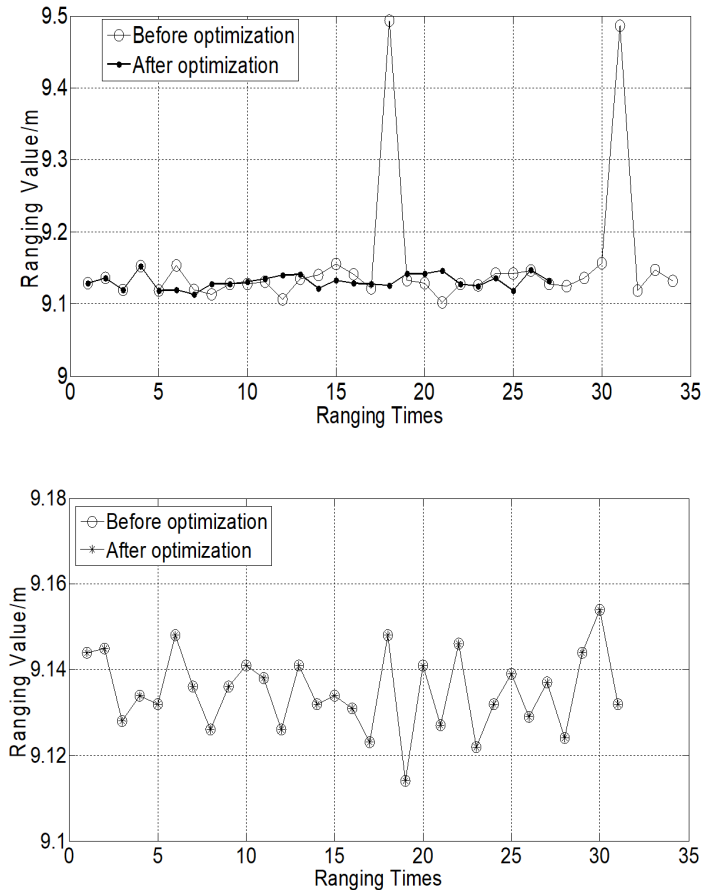


Fig. 3. Optimization results of edge detection

From Fig. 3, upper part, it can be seen that measured distance optimization method can eliminate the ranging value with obvious errors. All the ranging values after the elimination are located between 9.1 m and 9.15 m. Excluded values usually contain NLOS type data and other error effects. In addition, we can see that measured distance optimization method eliminates a total of seven ranging data, including two larger data error which can be visually seen from the figure. After the removal, overall data is very concentrated.

It can be seen from Fig. 3, bottom part, that the data obtained by the test itself is more concentrated, located between 9.11 m and 9.16 m. Standard deviation in Fig. 3,

upper part, is 0.0864 m, while it the bottom part it is 0.0097 m. So the measured distance optimization method can effectively improve the distance accuracy.

In addition, from both parts of Fig. 3 it can be found, because the P440 module has been processed ranging data itself, that if UWB measured turned failure then it will return 0, and the 0 data will not be considered. That is why there is a difference in the number of distance data from the two tests.

#### *4.2. Analysis of 3D positioning results*

Four known points are selected for experiment, each known point is continuously observed for a period of time. The distance intersection of space algorithm of the optimal distance is used to solve the three-dimensional coordinates for two consecutive seconds. The errors of these coordinates and the known precise coordinates are solved, as shown in Table 1.

Table 1. Test results of insulated resistance value (k $\Omega$ )

Point number	Axis	Mean value (m)	True value (m)	Standard deviation (cm)	Average point error (cm)
1	X	3.7262	3.749	0.0039	6.11
	Y	1.6907	1.635	0.0072	
	Z	1.6593	1.670	0.0061	
2	X	5.6325	5.685	0.0042	7.67
	Y	1.6819	1.637	0.0101	
	Z	1.7074	1.674	0.0082	
3	X	3.7777	3.751	0.0049	5.77
	Y	3.4606	3.439	0.0110	
	Z	1.6216	1.668	0.0183	
4	X	5.7034	5.682	0.0032	3.91
	Y	3.4267	3.444	0.0033	
	Z	1.6432	1.671	0.0048	

It can be seen from Table 1 that the average of several measurements is close to the true value, and the standard deviation of each solved value is small, indicating that each solved results has a low degree of dispersion, and results can be well gathered near the true value.

Limited to space, take point 1 as an example, the three-axis error and point error shown in Fig. 4. It can be seen from Fig. 4 that the three-axis error and point error are not randomly distributed along the zero, there is a certain systematic error that may be caused in the optimization algorithm. At the same time, it is found that the

point error is in the range of 8 cm, and the precision is high.

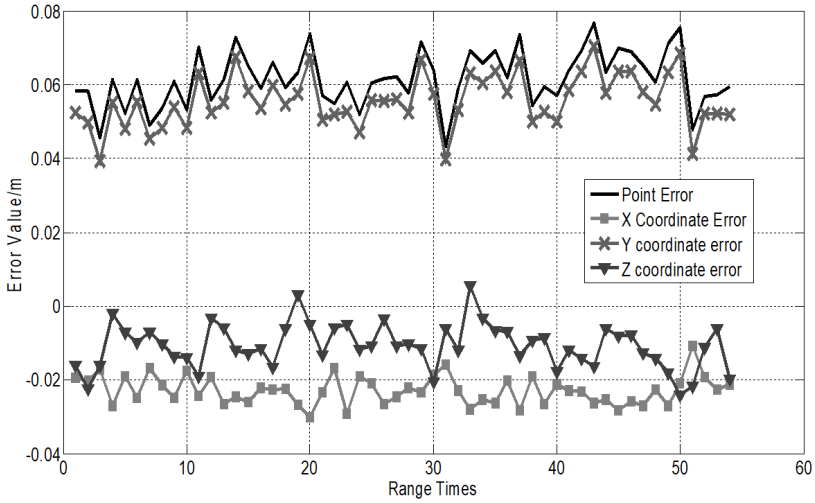


Fig. 4. Three-axis error and point error

Point 1 was continuously tested 41-times, and the results are shown in Fig. 5. It is considered that the positioning accuracy is high,  $x$ -axis value is between 3.71 m and 3.74 m,  $y$ -axis is between 1.67 m and 1.71 m, and  $z$ -axis is between 1.64 m and 1.68 m.

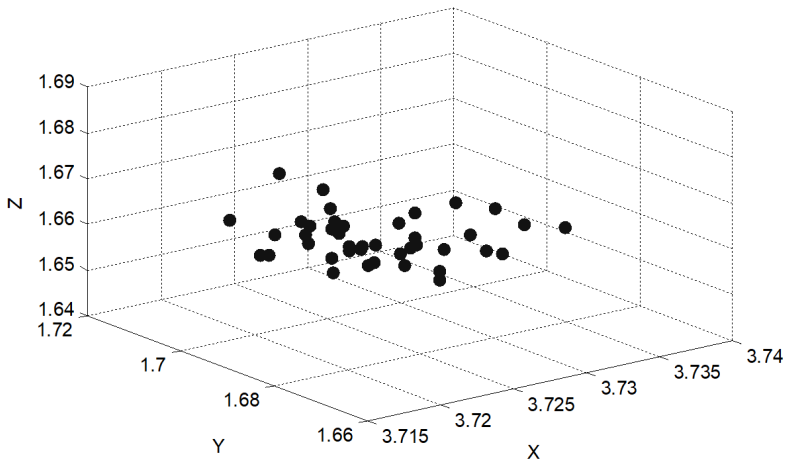


Fig. 5. Test results of point 1

## 5. Conclusion

In order to improve the localization accuracy of UWB, an improved UWB space location method is proposed in this paper. The method optimizes the ranging, and then use the distance intersection of space method to solve 3D coordinates.

Based on continuous 2 seconds of data processing, the method optimizes the ranging and effectively improves the accuracy of ranging. The space location algorithm in the method is simple and practical, and its computation cost is small. Tag's 3D coordinates can be solved by only three base stations, which saves the hardware cost. It can be applied to large-scale warehouse equipment management and other application scenarios, it may not suitable for real-time demanding applications.

In addition, a future study on ranging optimization method, such as study the empirical model, to eliminate system errors, which can improve the ranging accuracy for static positioning to provide a higher positioning accuracy, remains as a future work.

## References

- [1] R. MAALEK, F. SADEGHPOUR: *Accuracy assessment of ultra-wide band technology in locating dynamic resources in indoor scenarios*. *Automation in Construction* 63 (2016), 12–26.
- [2] R. A. SANTOS, A. C. SODRÉ, S. E. BARBIN: *A low-profile printed antenna for UWB applications*. Proc. International Conference on Electromagnetics in Advanced Applications (ICEAA), 19–23 September 2016, Cairns, QLD, Australia, IEEE Conference Publications (2016), 905–908.
- [3] G. YANJING, A. LO, I. NIEMEGEERS: *A survey of indoor positioning systems for wireless personal networks*. *IEEE Communications Surveys & Tutorials* 11 (2009), No. 1, 13–32.
- [4] X. SUI, G. YANG, Y. HAO, C. WANG, A. XU: *Dynamic positioning method based on TDOA in underground mines using UWB ranging*. *Journal of Navigation and Positioning* 4 (2016), No. 03, 10–14,34.
- [5] B. ALAVI, K. PAHLAVAN: *Modeling of the TOA-based distance measurement error using UWB indoor radio measurements*. *IEEE Communications Letters* 10 (2006), No. 4, 275–277.
- [6] B. SILVA, G. P. HANCKE: *IR-UWB-Based non-line-of-sight identification in harsh environments: Principles and challenges*. *IEEE Transactions on Industrial Informatics* 12 (2016), No. 3, 1188–1195.
- [7] X. LIANG, H. ZHANG, T. LV, X. CUI, T. A. GULLIVER: *NLOS identification approach based on energy block for 60GHz systems*. *International Journal of Database Theory and Application* 9 (2016), No. 9, 59–74.
- [8] X. LIU, Y. HUANG, Y. QIAN, J. WANG: *A TDOA localization algorithm based on sequential quadratic programming*. *SERSC Advanced Science and Technology Letters* 138 (2016), 134–139.
- [9] S. A. A. SHAHIDIAN, H. SOLTANIZADEH: *Path planning for two unmanned aerial vehicles in passive localization of radio sources*. *Aerospace Science and Technology* 58 (2016), 189–196.
- [10] E. OKAMOTO, M. HORIBA, K. NAKASHIMA, T. SHINOHARA, K. MATSUMURA: *Low-complexity indoor UWB localization scheme using particle swarm optimization*. *IEICE Nonlinear Theory and Its Applications* 6, (2015), No. 2, 194–206.

- [11] J. KHODJAEV, S. TEDESCO, B. O'FLYNN: *Improved NLOS error mitigation based on LTS algorithm*. PIER Progress In Electromagnetics Research Letters 58 (2016), 133–139.
- [12] L. LI, Z. WEN, Z. WANG: *Outlier detection and correction during the process of groundwater level monitoring base on pauta criterion with self-learning and smooth processing*. Proc. Asia Simulation Conference and SCS Autumn Simulation Multi-Conference, 8–11 October 2016, Beijing, China, Springer Singapore (2016), 497–503.
- [13] B. DAI, X. LÜ, X. LIU, Z. LI, : *A UWB-based four reference vectors compensation method applied on hazardous chemicals warehouse stacking positioning*. Journal of Chemical Industry and Engineering(China) 67 (2016), No. 03, 871–877.
- [14] M. NDOYE, J. M. M. ANDERSON, D. J. GREENE: *An MM-based algorithm for-regularized least-squares estimation with an application to ground penetrating radar image reconstruction*. IEEE Transactions on Image Processing 25 (2016), No. 5, 2206 to 2221.
- [15] A. LIU, Y. DU, H. SUN: *Research on positioning solutions of distance intersection applied with laser range-finder*. Modern Electronics Technique 38 (2015), No. 19, 24–32.

Received June 29, 2017